Direct numerical simulations of "on-demand" vortex generators — Mathematical formulation

By P. Koumoutsakos

1. Motivation and objectives

The objective of the present research is the development and application of efficient adaptive numerical algorithms for the study, via direct numerical simulations, of active vortex generators. We are using innovative computational schemes to investigate flows past complex configurations undergoing arbitrary motions. Some of the questions we try to answer are: Can and how may we control the dynamics of the wake? What is the importance of body shape and motion in the active control of the flow? What is the effect of three-dimensionality in laboratory experiments?

We are interested not only in coupling our results to ongoing, related experimental works, but furthermore to develop an extensive database relating the above mechanisms to the vortical wake structures with the long-range objective of developing feedback control mechanisms. This technology is very important to aircraft, ship, automotive, and other industries that require predictive capability for fluid mechanical problems. The results would have an impact in high angle of attack aerodynamics and help design ways to improve the efficiency of ships and submarines (maneuverability, vortex induced vibration, and noise).

2. Accomplishments

This is a preliminary report describing our numerical method and presenting results of direct numerical simulations of pertinent two-dimensional bluff body flows. Our final objective is the simulation of flows past the three dimensional configuration shown in Fig. 1a. At the first stage of this work, we are interested in the respective two-dimensional configuration (Fig. 1b). The results of these simulations would help us investigate the effects of three dimensionality in experiments and assess the role of two-dimensional vortical mechanisms.

2.1 Mathematical formulation - numerical method

Two-dimensional incompressible unsteady flow of a viscous fluid may be determined by the vorticity transport equation as

$$\frac{\partial \omega}{\partial t} + \mathbf{u} \cdot \nabla \omega = \nu \nabla^2 \omega \tag{1}$$

where $\mathbf{u}(\mathbf{x}, t)$ is the velocity, $\omega = \omega \,\widehat{\mathbf{e}_z} = \nabla \times \mathbf{u}$ the vorticity, and ν denotes the kinematic viscosity. For flow around a non-rotating flat plate, translating with velocity $\mathbf{U_b}(t)$, the velocity of the fluid ($\mathbf{u}$) on the surface of the body ($\mathbf{x_s}$) is equal to the velocity of the body:

$$\mathbf{u}(\mathbf{x_s}, t) = \mathbf{U_b(t)} \tag{1a}$$
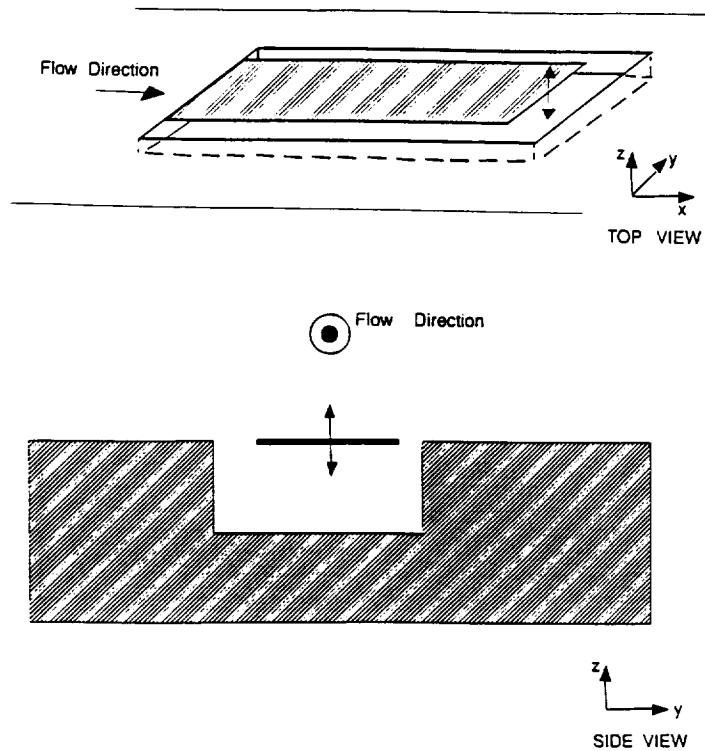
FIGURE 1. Definition sketch. Top view (a), front view (b).

At infinity we have:

$$u(x) \rightarrow U_\infty \qquad \text{as} \quad |x| \rightarrow \infty \tag{1b}$$

where U_∞ is the free stream velocity. Using the definition of the vorticity and the continuity ($\nabla \cdot u = 0$), it can be shown that u is related to ω by the following Poisson equation:

$$\nabla^2 u = -\nabla \times \omega . \tag{2}$$

The velocity-vorticity formulation helps in eliminating the pressure from the unknowns of the equations. However, for bounded domains, it introduces additional constraints in the kinematics of the flow field and requires the transformation of the velocity boundary conditions to vorticity form.

2.1.1 Particle/vortex methods

The present numerical method is based on the discretization of the above equations in a Lagrangian frame using particle (vortex) methods. The vorticity equation

Eq. 1 may be expressed in a Lagrangian formulation by solving for the vorticity-carrying fluid elements ($\mathbf{x_a}$) based on the following set of equations:

$$\frac{d\mathbf{x_a}}{dt} = \mathbf{u}(\mathbf{x_a}, t)$$
$$\frac{d\omega}{dt} = \nu \, \nabla^2 \omega \tag{3}$$

In the context of particle methods, it is desirable to replace the right-hand side of equations Eq. 3 by integral operators. These operators are discretized using the locations of the particles as quadrature points so that ultimately Eq. 3 is replaced by a set of O.D.E.'s whose solution is equivalent to the solution of the original set of equations. To this effect the velocity field may be determined by the vorticity field using the Green's function formulation for the solution of Poisson's equation (Eq. 2).

$$\mathbf{u} = = -\frac{1}{2\pi} \int \mathbf{K}(\mathbf{x} - \mathbf{y}) \times \omega \, d\mathbf{y} + \mathbf{U_0}(\mathbf{x}, t) \tag{4}$$

where $\mathbf{U_0}(\mathbf{x}, t)$ contains the contribution from the solid body rotation and $\mathbf{U_\infty}$, and $\mathbf{K}(\mathbf{z}) = \mathbf{z}/|\mathbf{z}|^2$. The use of the Biot-Savart law to compute the velocity field guarantees the enforcement of the boundary condition at infinity.

The Laplacian operator may be approximated by an integral operator (Degond and Mas-Gallic, 1989) as well so that:

$$\nabla^2 \omega \approx \int G_\epsilon(|\mathbf{x} - \mathbf{y}|) \, [\omega(\mathbf{x}) - \omega(\mathbf{y})] \, d\mathbf{y} \tag{5}$$

where, in this paper, G_ϵ is taken to be $G_\epsilon(\mathbf{z}) = (2/\pi\epsilon^2) \, exp(-|\mathbf{z}|^2/2\epsilon^2)$. The boundary condition Eq. 1a is enforced by formulating the physical mechanism it describes. The surface of the plate is the source of vorticity that enters the flow. A vorticity flux ($\partial\omega/\partial n$) may be determined on the boundary in a way that ensures Eq. 1a is satisfied. Here a fractional step algorithm is presented that allows for the calculation of this vorticity flux (see also Koumoutsakos *et al.* 1993). It is shown then that this mechanism of vorticity generation can be expressed by an integral operator as well:

$$\frac{d\omega}{dt} = \int H(\mathbf{x}, \mathbf{y}) \, \frac{\partial\omega}{\partial n}(\mathbf{y}) \, d\mathbf{y} \tag{6}$$

where the kernel H is developed in Section 3. Using the above integral representations for the right-hand side of Eq. 3, we obtain the following set of equations.

$$\frac{d\mathbf{x_a}}{dt} = -\frac{1}{2\pi} \int \mathbf{K}(\mathbf{x_a} - \mathbf{y}) \times \omega \, d\mathbf{y} + \mathbf{U_0}(\mathbf{x_a}, t)$$
$$\frac{d\omega}{dt} \approx \nu \int G_\epsilon(|\mathbf{x_a} - \mathbf{y}|) \, [\omega(\mathbf{x_a}) - \omega(\mathbf{y})] \, d\mathbf{y} \tag{7}$$
$$\frac{d\omega}{dt} \approx \nu \int H(\mathbf{x_a}, \mathbf{y}) \, \frac{\partial\omega}{\partial n}(\mathbf{y}) \, d\mathbf{y}$$

In vortex methods, the vorticity field is considered as a discrete sum of the individual vorticity fields of the particles, having core radius ϵ, strength $\Gamma(t)$, and an individual distribution of vorticity determined by the function η_ϵ so that:

$$\omega(\mathbf{x},t) = \sum_{n=1}^{N} \Gamma_n(t)\, \eta_\epsilon(\mathbf{x} - \mathbf{x}_n(t)) \tag{8}$$

When this expression for the vorticity is substituted in Eq. 7, the singular integral operators K,G are convolved with the smooth function η_ϵ and are replaced by smooth operators K_ϵ, G_ϵ. These integrals are subsequently discretized using a quadrature having as quadrature points the locations of the particles. Assuming that each particle occupies a region of area h^2 and that the shape of the body is discretized by M panels, then algorithmically the method may be expressed as:

$$
\begin{aligned}
\frac{d\mathbf{x}_i}{dt} &= -\frac{1}{2\pi}\sum_{j=1}^{N} \Gamma_j\, K_\epsilon(\mathbf{x}_i - \mathbf{x}_j) + \mathbf{U}_0(\mathbf{x}_i, t) \\[4pt]
\frac{d\Gamma_i}{dt} &= \nu \sum_{j=1}^{N}[\Gamma_j - \Gamma_i]\, G_\epsilon(|\mathbf{x}_i - \mathbf{x}_j|) \\[4pt]
\frac{d\Gamma_i}{dt} &= \nu \sum_{m=1}^{M} H(\mathbf{x}_i, \mathbf{x}_m)\, \frac{\partial\omega}{\partial n}(\mathbf{x}_m) \\[4pt]
\Gamma_i(0) &= \omega(\mathbf{x}_i, 0)\, h^2 \qquad i = 1, 2, \ldots, N
\end{aligned}
\tag{9}
$$

The Lagrangian representation of the convective terms avoids many difficulties associated with its discretization on an Eulerian mesh such as excess numerical diffusion. However the straightforward method of computing the right-hand side of (Eq. 8), using (Eq. 9) for every particle, requires $\mathcal{O}(N^2)$ operations for N vortex elements. Recently fast methods have been developed that have operation counts of $\mathcal{O}(N)$ (Greengard and Rohklin, 1987). In the present scheme the efficient vectorization of the $\mathcal{O}(N)$ scheme allows for computations with one CPU minute per velocity evaluation for one million vortices on a single processor of a CRAY YMP. The accuracy of the method relies on the accuracy of the quadrature rule as information needs to be gathered from the possibly scattered particle positions. The convergence properties of vortex methods with a finite core dictate that the particles must overlap (i.e. $h < \epsilon$) at all times (Beale, 1986). However the local strain field of the flow may distort the particle locations, thus producing particle clustering in one direction accompanied by an expansion in another direction, similar to that which would occur around a hyperbolic stagnation point in a steady flow. When such a situation occurs the particle locations have to be re-initialized (remeshed) onto a uniform grid while interpolating the old vorticity on the new particle locations. In our algorithm we use a nine-point scheme to perform this remeshing, conserving the circulation as well as the linear and angular momentum of the vorticity field. See Koumoutsakos (1993) for further discussion.

2.2 A fractional step algorithm - boundary conditions

The no-slip boundary condition accounts for the generation of vorticity on the surface of the body. The surface of the body acts as a source of vorticity (Lighthill, 1963), and the task is to relate this vorticity flux on the surface of the body to the no-slip condition. This is achieved by appropriately coupling the kinematic and dynamic constraints of the flow. The present methodology was first proposed by Schmall and Kinney (1974) and is implemented here in a fractional step algorithm.

In the present formulation Eq. 9 are not integrated simultaneously in time, but instead a fractional step algorithm is employed. The governing equations are solved via a splitting scheme that accommodates the enforcement of the boundary conditions. For a non-zero thickness body the enforcement of the no-tangency flow implies the enforcement of the no-through flow as well (Koumoutsakos, 1993). This is not the case, however, for the zero thickness flat plate, as one has to account explicitly for the no-through flow boundary condition.

Let us assume that at the n-th time step (corresponding to time $t - \delta t$) the vorticity field has been computed (respecting the no-slip boundary condition) and we seek to advance the solution to the next time step (time t). The following two-step procedure is implemented:

- **Step 1:** Using as initial conditions $f(\mathbf{x}) = \omega^n(\mathbf{x}^n, n\delta t)$ we solve:

$$
\begin{aligned}
\omega_t + \mathbf{u} \cdot \nabla\omega &= \nu\nabla^2\omega &&\text{in } \mathcal{D} \times [t - \delta t, t] \\
\omega(\mathbf{x}, t - \delta t) &= f(\mathbf{x}) &&\text{in } \mathcal{D}
\end{aligned}
\tag{10}
$$

where $\mathcal{D}$ denotes the flow domain exterior to the body surface $\partial\mathcal{D}$. Particles are advanced via the Biot-Savart law, and their strength is modified based on the scheme of Particle Strength Exchange.

Algorithmically then Step 1 may be expressed as:

$$
\begin{aligned}
\frac{d\mathbf{x}}{dt} &= u^n(\mathbf{x}^n, n\delta t) \\
\frac{d\omega'_1}{dt} &= \nu\nabla^2\omega'_1
\end{aligned}
\tag{11}
$$

At the end of Step 1 a vorticity field ω'_1 has been established in the fluid.

- **Step 2:**

The boundary conditions are enforced in this stage by a vorticity (not particle) creation algorithm.

2.2.1 Simply connected domain - flat plate

Without loss of generality we assume that the plate surface lies along the x-axis at $y = 0$ and between $-L/2 \leq x \leq L/2$. First, in order to enforce the **no-through** flow boundary condition, a vortex sheet of strength $\kappa(\xi)$ is distributed on the plate surface. The strength of this vortex sheet is then determined by the solution of the following integral equation:

$$
\int_{-L/2}^{L/2} \frac{\kappa(\xi)}{x - \xi} d\xi = \mathbf{u}_n(x)
\tag{12}
$$

where $u_n(x)$ is the velocity normal to the surface of the plate. The above integral equation is singular as it admits more than one solution. A unique solution is obtained by enforcing the conservation of circulation (note that in airfoil theory κ is uniquely determined by enforcing the Kutta condition)

$$\int_{-L/2}^{L/2} \kappa(\xi)d\xi = -\int \omega(\mathbf{x})d\mathbf{x} \tag{13}$$

Introducing the transformation $\theta = cos^{-1}(\frac{2y}{L})$ and using the orthogonality of a Fourier series expansion for $\kappa(\theta)$, (Batchelor, 1967) over the interval $[0, \pi]$, we obtain that at each instant of time:

$$\kappa(\theta) = -(A_0 + 2\sin\beta)\frac{\cos\theta}{\sin\theta} + \frac{C}{\sin\theta} + 2\sum_{m=1}^{\infty} A_m \sin(m\theta) \tag{14}$$

where:

$$A_m = \frac{2}{\pi}\int_0^{\pi} u_n(\theta)\cos(m\theta)d\theta \qquad \text{for} m = 0, 1, \ldots, \infty \tag{15}$$

and C is determined by enforcing the conservation of circulation (Eq. 13):

$$C = \frac{2\Gamma}{\pi L} + A_1 \tag{16}$$

A finite number of terms (P) is retained in the infinite series Eq. 14 in the numerical implementation of this method. Note also that the expression in Eq. 14 has built in the singularity of the vortex sheet at the tips of the plate. The enforcement of the no-through flow does not imply the enforcement of the no-slip condition for the zero thickness flat plate. A tangential velocity $u_t(x)$ may be computed along the plate surface due to the vortices in the wake. By taking the limit of Eq. 12 a vortex sheet of strength γ is observed on each side of the plate as:

$$\begin{aligned} \gamma(y = 0^-, x) &= -\frac{1}{2}\kappa(x) + u_t(x) \\ \gamma(y = 0^+, x) &= +\frac{1}{2}\kappa(x) + u_t(x) \end{aligned} \tag{17}$$

In order to enforce the **no-slip** condition then, in the context of the present algorithm we need to eliminate the spurious vortex sheet (κ) and the tangential velocity on the surface of the plate.

2.2.2 Doubly connected domain - vortex generators

For a doubly connected domain as that shown in Fig. 1b, the potential flow problem needs to be modified. For an open domain such as that exterior to the cavity (in the absence of the flat plate), in order to enforce the no-through flow boundary condition we require that the tangent flow on the interior surface of the boundary vanishes. Unlike the case of a closed body, no additional constraint needs

to be imposed for the solution of the respective integral equation (Koumoutsakos and Leonard, 1989).

For the combined configuration the resulting integral equation is then:

$$\int_{-L/2}^{L/2} \frac{\kappa(\xi)}{\mathbf{x}_p - \xi} d\xi + \int_{-\infty}^{\infty} \gamma_w(\zeta) \frac{\partial}{\partial s(\mathbf{x}_p)} Log|\zeta - \mathbf{x}_p| d\zeta = \mathbf{u}_n(\mathbf{x}_p) \qquad (18a)$$

$$\int_{-L/2}^{L/2} \kappa(\xi, t) d\xi = -\nu \int_0^t \int_{-L/2}^{L/2} \frac{\partial \omega(\mathbf{x}_p, T)}{\partial n(\mathbf{x}_p)} d\mathbf{x}_p \, dT \qquad (18b)$$

$$\int_{-L/2}^{L/2} \kappa(\xi) \frac{\partial}{\partial n(\zeta)} Log|\zeta - \xi| d\xi + \int_{-\infty}^{\infty} \gamma_w(\zeta') \frac{\partial}{\partial n(\zeta)} Log|\zeta - \zeta'| d\zeta' = \mathbf{u}_t(\zeta) \quad (18c)$$

where $\kappa(\xi), \mathbf{x}_p$ and $\gamma_w(\zeta), \zeta$ denote vortex sheets and location of points on the surface of the plate and the cavity respectively.

The above set of equations, when discretized using a panel method, results in a well posed system of equations which can be solved iteratively or by direct LU decomposition (if storage is not a limiting factor).

The spurious vortex sheet (γ) that is observed on the surface of the body may then be translated to a vorticity flux (Koumoutsakos and Leonard (1994)).

$$\nu \frac{\partial \omega}{\partial n}(x) = \frac{\gamma}{\delta t}(x) \qquad \text{on } \partial \mathcal{D} \qquad (19)$$

The computed vorticity flux generates vorticity in the fluid. The vorticity field is augmented by this viscous mechanism as described by the following set of equations:

$$\begin{aligned} \frac{\partial \omega_2'}{\partial t} - \nu \nabla^2 \omega_2' &= 0 & \text{in } \mathcal{D} \times [t - \delta t, t] \\ \omega_2'(\mathbf{x}, t - \delta t) &= 0 & \text{in } \mathcal{D} \\ \nu \frac{\partial \omega_2'}{\partial n} &= \frac{\gamma(\omega_1')}{\delta t} & \text{on } \partial \mathcal{D} \end{aligned} \qquad (20)$$

Note that the diffusion equation is solved here with homogeneous initial conditions as the initial vorticity field was taken into account in the previous substep. The solution at Step 2 is a vorticity field ω_2', which we superimpose onto the solution of Step 1 to obtain the vorticity distribution at the next time step

$$\omega^{n+1} = \omega_1' + \omega_2' \qquad (21)$$

3. Results

We have conducted a computational study of the unsteady flow behind a zero thickness plate started impulsively or uniformly accelerated normal to the flow.
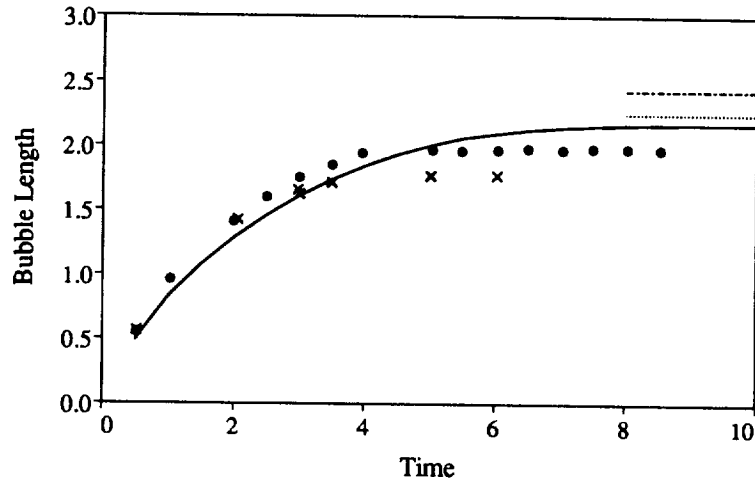
FIGURE 2.   Evolution of the recirculating bubble for Re = 20. ———— : Present computations, • ,× : Experiments (Coutanceau and Launay)for blockage ratios of 0.1 and 0.15 respectively. Theory (Steady State Results): —·—— : Dennis and Qiang, ········ : Ingham and Tang.

For the impulsively started plate the present results complement related experimental works while providing quantities such as the vorticity of the flow field and the forces experienced by the body. The development of the flow is similar for all the Reynolds numbers that were simulated (20 to 1000). The separating shear layer rolls up into a vortex in the lee of the plate, inducing initially a region of secondary vorticity. Diffusion acts to increase the width of the shear layer and reduce the strength of the vortex resulting in a stable configuration. In Fig. 2 we present the results of the present computations for the length of the recirculating bubble for Re=20 and compare with existing experimental and theoretical works. The discrepancies may be attributed to the different treatment of the boundary conditions from the calculations of the steady state results and to the finite blockage ratio in the experiments. A different behavior is observed for the separating shear layer of a uniformly accelerated plate(U = a t). The continuous increase of the shear flow overcomes the effects of diffusion, increasing the strength of the separating shear layer and inducing a Kelvin-Helmholtz type instability. The wavelength and the onset of this instability depends on the acceleration of the plate. The present simulations are the first to confirm related experimental evidence on the formation of vortex centers along the separating shear layers of an accelerating flat plate (Fig.3). Such undulations have been attributed to experimental defects, but the present simulations suggest that this is an intrinsic behavior of the flow. Finally the drag coefficient of the plate is shown to scale due to the similarity in the inviscid development of the flow.

An extensive study of these flows for various Re numbers and acceleration rates may be found in Koumoutsakos (1994).
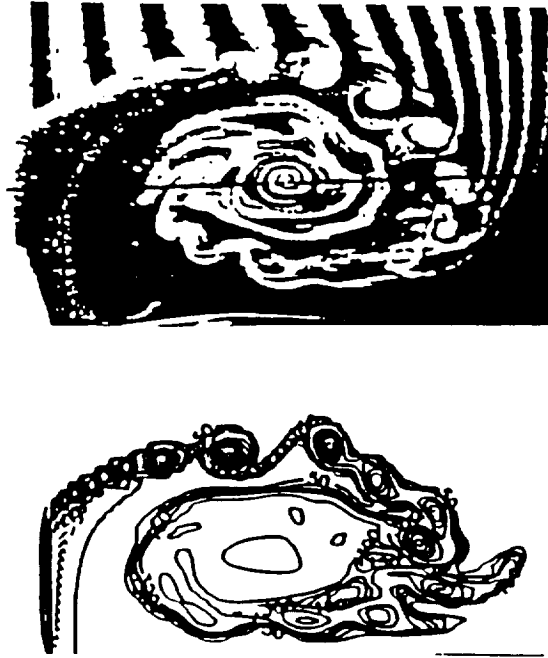
FIGURE 3. Flow past an accelerating flat plate. Top: Experimental results from Lian and Huang (1989) for $\alpha = aL^3/\nu^2 = 24.51 \times 10^6$ at $T^* = at^2/L = 4.37$. Bottom: Computational results. Equivorticity Contours for $\alpha = 1.68 \times 10^6$ at $T^* = 6.25$.

4. Future plans

We are currently at the final stages of development of our code for the study of flows involving the doubly connected configuration shown in Fig. 1b. We are interested in investigating the role of three dimensionality in the experiments and determining the role of two-dimensional vortical structures. We will be investigating possible control mechanisms with the long-range objective of developing feedback control mechanisms.

Our final goal is full three-dimensional direct numerical simulations to complement the ongoing experimental investigations. We may use existing algorithms or algorithms under development or proceed to extend the present computational technique to three-dimensional flows. In particular, research would be directed in the development of fast solutions of integral equations in three dimensions (with possible multi-disciplinary applications) and the process of restoring the Lagrangian computational grid. Of particular interest would be the coupling of the present Lagrangian method with large-eddy simulation (LES) methodologies.

Acknowledgments

I wish to acknowledge many extensive and enlightening discussions with Professor Anthony Leonard and Mr. Douglas Shiels of the Department of Aeronautics at the California Institute of Technology.

REFERENCES

BEALE, J. T. 1994 On the accuracy of vortex methods at large times, *Proc. Workshop on Comp. Fluid Dyn. and React. Gas Flows*. IMA, Univ. of Minnesota.

DENNIS, S. C. R., QIANG, W., COUTANCEAU, M., &LAUNAY, J-L. 1993 Viscous flow normal to a flat plate at moderate Reynolds numbers. *J. Fluid Mech.* **248**, 605-635.

DEGOND, P. & MAS-GALLIC, S. 1989 The Weighted Particle Method for Convection-Diffusion Equations, Part I: The Case of an Isotropic Viscosity, Part II: The Anisotropic Case. *Math. Comput.* **53**, 485-526.

GREENGARD, L. AND ROHKLIN, V. 1987 A fast algorithm for particle simulations. *J. Comput. Phys.* **73**, 325-348.

INGHAM, T. B. AND TANG, T. 1991 Steady two-dimensional flow past a normal flat plate. *J. of Applied Math. and Phys. (ZAMP).* **42**, 584.

KOUMOUTSAKOS, P. AND LEONARD A. 1989 Improved Boundary Integral Method for Inviscid Boundary Condition Applications. *AIAA J.* **31(2)**, 401-404.

KOUMOUTSAKOS, P. 1993 Direct Numerical Simulations of Unsteady Separated Flows Using Vortex Methods. *Ph.D. Thesis*. California Institute of Technology.

KOUMOUTSAKOS, P., LEONARD, A. AND PEPIN, F. 1994 Boundary Conditions for Viscous Vortex Methods. *J. of Comput. Phys.* **113**, 52-61.

KOUMOUTSAKOS, P. & LEONARD, A. 1994 High Resolution simulations of the flow past an impulsively started cylinder. *J. Fluid Mech.* To appear.

KOUMOUTSAKOS, P. 1994 Simulations of the Viscous Flow Normal to a Zero Thickness Flat Plate. *J. Fluid Mech.* Submitted.

LIGHTHILL, M. J. 1963 *Introduction. Boundary Layer Theory*. J. Rosenhead Ed., Oxford Univ. Press, NY. 54-61.

LIAN, Q. X. & HUANG, Z. 1989 Starting flow and structures of the starting vortex behind bluff bodies with sharp edges. *Experiments in Fluids.* **8**, 95.

SCHMALL, R. A. & KINNEY, R. B. 1974 Numerical Study of Unsteady Viscous Flow past a lifting plate. *AIAA J.* **12** (11), 1566.